BIOCHEMISTRY
including biophysical chemistry & molecular biology
Article

Biochemistry **2010,** *49,* 6727–6736 6727
DOI: 10.1021/bi100886z

Synthesis of Glu-tRNA^{Gln} by Engineered and Natural Aminoacyl-tRNA Synthetases†

Annia Rodríguez-Hernández, Hari Bhaskaran, Andrew Hadd, and John J. Perona*

Department of Chemistry and Biochemistry and Interdepartmental Program in Biomolecular Science and Engineering, University of California, Santa Barbara, California 93106-9510

Received June 1, 2010; Revised Manuscript Received July 8, 2010

ABSTRACT: A protein engineering approach to delineating which distinct elements of homologous tRNA synthetase architectures are responsible for divergent RNA−amino acid pairing specificities is described. Previously, we constructed a hybrid enzyme in which 23 amino acids from the catalytic domain of *Escherichia coli* glutaminyl-tRNA synthetase (GlnRS) were replaced with the corresponding residues of human glutamyl-tRNA synthetase (GluRS). The engineered hybrid (GlnRS S1/L1/L2) synthesizes Glu-tRNA^{Gln} more than 10^4-fold more efficiently than GlnRS. Detailed comparison of kinetic parameters between GlnRS S1/L1/L2 and the naturally occurring *Methanothermobacter thermautotrophicus* GluRSND, which is also capable of Glu-tRNA^{Gln} synthesis, now shows that both k_{cat} and K_m for glutamate are recapitulated in the engineered enzyme, but that K_m for tRNA is 200-fold higher. Thus, the simultaneous optimization of paired amino acid and tRNA binding sites found in a naturally occurring enzyme is not recapitulated in a hybrid that is successfully engineered for amino acid complementarity. We infer that the GlnRS architecture has differentiated to match only cognate amino acid−RNA pairs, and that the substrate selection functions do not operate independently of each other. Design and characterization of four additional hybrids identify further residues involved in improving complementarity for glutamate and in communicating between amino acid and tRNA binding sites. The robust catalytic function demonstrated in this engineered system offers a novel platform for exploring the stereochemical origins of coding as a property of the ancient Rossmann fold.

Aminoacyl-tRNA synthetases translate the genetic code by catalyzing the specific pairing of amino acids and tRNAs (*1*). In a common two-step reaction pathway, an activated aminoacyl adenylate is first synthesized from the amino acid and ATP. In the second step, one of the hydroxyl groups located on the 3′-terminal ribose sugar of the tRNA attacks the carbonyl carbon of the mixed anhydride linkage of the adenylate intermediate, generating aminoacyl-tRNA with release of AMP. The tRNA synthetases specific for glutamine, glutamate, lysine, and arginine (GlnRS,[1] GluRS, class I LysRS, and ArgRS, respectively) form a subgroup that function only as ribonucleoprotein (RNP) catalysts. These four enzymes, which possess a common Rossmann fold catalytic domain, cannot detectably synthesize the aminoacyl adenylate intermediate in the absence of tRNA.

The glutamyl- and glutaminyl-tRNA synthetase families share a common evolutionary history. Phylogenetic analysis has shown that an ancestral GluRS enzyme possessing a catalytic Rossmann fold acquired distinct tRNA binding modules upon separation of the bacterial and archaeal domains (*2*, *3*). Bacterial GluRS acquired an α-helical anticodon-binding domain, as exemplified by crystal structures of the *Thermus thermophilus* enzyme (*4*). In contrast, archaeal GluRS acquired anticodon domains that form β-barrel structures. After the divergence of the eukaryal lineage, duplication of the gene encoding GluRS allowed differentiation of GlnRS for the first time. Thus, cytoplasmic GluRS and GlnRS from eukaryotes are of the β-class. Subsequently, horizontal transfer of eukaryotic GlnRS to a number of bacterial phyla established the enzyme in that domain (*5*). In these bacteria, then, α-class GluRS enzymes coexist with β-class GlnRS enzymes, and the enzymes are relatively distantly related. The β-barrel anticodon domain structure of β-class enzymes was first revealed by the crystal structure of *Escherichia coli* GlnRS (*6*).

Most GluRS enzymes in organisms that lack GlnRS are nondiscriminating (GluRSND): they are able to synthesize both Glu-tRNA^{Glu} and Glu-tRNA^{Gln} (*7*, *8*). The Glu-tRNA^{Gln} is then converted to Gln-tRNA^{Gln} by ATP and tRNA-dependent amidotransferase enzymes (*9*). Thus, these organisms are able to use glutamine as an encoded amino acid despite the absence of GlnRS. GluRSND enzymes are found in all archaea, in bacteria that lack GlnRS, and in eukaryotic organelles (*10*, *11*). A GluRSND enzyme may be either of the α-class (bacteria) or β-class (archaea): crystal structures of both varieties have been reported (*12*, *13*). In some bacteria, GluRS gene duplication has also occurred. One GluRS enzyme in these organisms appears to be dedicated to Glu-tRNA^{Gln} synthesis alone and, hence, may represent a third class of GluRS specificity beyond the discriminating (GluRS^{D}) and nondiscriminating (GluRSND) enzymes (*14*, *15*). This more recently recognized GluRS variety, characterized from *Helicobacter pylori* and *Acidothiobacillus ferrooxidans*, has been termed GluRS2.

†Supported by Grant RO1GM063713 from the National Institutes of Health (to J.J.P.). A.R.-H. thanks the National Council for Science and Technology (CONACYT-Mexico) for financial support during the development of these experiments.

*To whom correspondence should be addressed: Department of Chemistry and Biochemistry, University of California, Santa Barbara, CA 93106-9510. Telephone: (805) 893-7389. Fax: (805) 893-4120. E-mail: perona@chem.ucsb.edu.

[1]Abbreviations: GlnRS, glutaminyl-tRNA synthetase; GluRS, glutamyl-tRNA synthetase; LysRS, lysyl-tRNA synthetase; ArgRS, arginyl-tRNA synthetase; IleRS, isoleucyl-tRNA synthetase; WT, wild-type; RNP, ribonucleoprotein; SDS, sodium dodecyl sulfate; K_m(AA), K_m value for the amino acid; K_m(Glu), K_m value for Glu; k_{cat}/K_m[AA], k_{cat}/K_m value for the amino acid; K_m[tRNA], K_m value for the tRNA.

Published on Web 07/09/2010

We have been interested in the origins of amino acid specificity in the related GluRS and GlnRS enzyme families (jointly termed the GlxRS family). Because substantial evidence for the well-studied *E. coli* GlnRS suggests that the tRNA and amino acid binding are interdependent (*16*−*19*), and because all GlxRS enzymes are thought to function as RNP enzymes, we have also developed the notion that certain tRNA nucleotides may assist the protein active site in selecting the proper amino acid (*20*). To examine the origins of amino acid discrimination among GlxRS enzymes, we introduced amino acids from the primary amino acid binding site of the evolutionarily related β-class human GluRS, into *E. coli* GlnRS. The resulting enzyme (GlnRS C229R/Q255I/S227A/Y233F) catalyzes Glu-tRNA^{Gln} synthesis 20-fold more efficiently than WT GlnRS, as judged from measurements of k_{cat} and K_m for glutamate [K_m(Glu)] (*20*). Further introduction of two distal surface loops bridging core secondary structural elements of the Rossmann fold then produced a hybrid enzyme (GlnRS S1/L1/L2) that synthesizes Glu-tRNA^{Gln} 1.6×10^4-fold faster than WT GlnRS (*21*), with a K_m(Glu) reduced by at least 130-fold (Figure 1A). However, k_{cat}/K_m with respect to glutamate, for aminoacylation by this hybrid enzyme, remains 800-fold reduced compared with that of cognate aminoacylation by WT GlnRS. The hybrid enzyme is completely inactive in the synthesis of Gln-tRNA^{Gln}, indicating that a bona fide switch in specificity has occurred.

The GlnRS S1/L1/L2 enzyme provides an experimental platform for exploring how the evolutionarily related GlnRS and GluRS sequences have become differentiated for selective pairing of cognate amino acid and tRNA. One important question concerns whether amino acid selectivity in the GlxRS family is associated entirely with the protein component of the RNP. Given the requirement for tRNA in aminoacyl adenylate synthesis, a plausible alternative hypothesis is that certain tRNA nucleotides function to help exclude noncognate amino acid substrates. The idea that particular tRNA nucleotides may assist amino acid discrimination has also been considered in the context of amino acid editing by IleRS (*22*).

We have performed a number of experiments to further test the notion that differentiation of the GluRS and GlnRS protein structures alone may provide selectivity for the amino acid substrate, in the context of efficient aminoacylation. Mutations were introduced at four other positions within the second half of the Rossmann fold of the GlnRS S1/L1/L2 hybrid, to examine the contribution of additional amino acids and to assess whether noncomplementarity with adjacent regions of GlnRS might mask higher catalytic efficiency. The ability of the hybrid enzymes to provide effective complementarity for tRNA was assessed by measuring tRNA K_m values and by examining the role of GlnRS Thr231 in a structural element bridging the amino acid and tRNA binding sites. Finally, we address the important question of how to benchmark the activities of the hybrid enzymes, by measuring steady-state kinetic parameters for Glu-tRNA^{Gln} synthesis by a naturally occurring GluRSND from the β-class, and by comparing these values to those of the hybrids and of other GluRS enzymes.

EXPERIMENTAL PROCEDURES

Enzyme Construction and Purification. Mutations in the gene encoding GlnRS S1/L1/L2 containing a C-terminal hexahistidine affinity tag were constructed using the Quikchange protocol (Stratagene) and were confirmed by DNA sequencing. Expression of all *E. coli* GlnRS mutants studied here was achieved in the context of an N-terminal signal sequence tag directing the protein to the periplasm; this added tag is without effect on the steady-state kinetic parameters of WT GlnRS (*20*). Mutants were expressed as N-terminal fusions with the leader sequence of the bacterial fd gene III protein (Invitrogen). As described for GlnRS S1/L1 and GlnRS S1/L1/L2, high-level expression of the mutants was achieved by addition of 1 mM IPTG and 10 mM β-mercaptoethanol to the culture at the time of induction ($A_{600} \sim 0.4$). Purification of the mutants by affinity chromatography on a nickel resin yielded enzyme preparations that were >98% pure, as judged by SDS−polyacrylamide gel electrophoresis. The hybrid enzymes were stored at high concentrations at −20 °C, in a buffer containing 50 mM NaCl, 50 mM potassium phosphate (pH 7.2), 5 mM β-mercaptoethanol, and 50% glycerol. Enzymes were quantitated on the basis of an E_{280}[1 mg/mL] of 1.06.

The *Methanothermobacter thermautotrophicus* GluRSND gene cloned into a pCYB1 vector (New England Biolabs) was the generous gift from K. Sheppard and D. Söll. The enzyme was expressed in pLysS Rosetta cell and purified as described previously (*23*). Briefly, the cells were grown at 37 °C to an A_{600} of 0.8, induced with 0.5 mM IPTG, and allowed to grow overnight at 25 °C. The cells from 1 L of saturated culture were centrifuged and resuspended in 35 mL of lysis buffer containing 20 mM sodium Hepes (pH 8.5) and 500 mM NaCl, followed by addition of 150 μg of DNase I, 50 mg of lysozyme, and 1 pellet of protease inhibitor (Complete Mini, EDTA-free protease inhibitor cocktail tablets, Roche Diagnostics, GmbH). The cells were sonicated for 5 min with an alternating 2 s pulse on and pulse off mode using a Branson (Danbury, CT) 450 digital sonicator. The cell-free lysate was then centrifuged at 15000 rpm for 45 min and the supernatant applied to a pre-equilibrated Chitin resin. GluRSND was cleaved from the column by overnight incubation with 50 mM DTT at 37 °C; recovered material was dialyzed against and stored in a buffer containing 25 mM Hepes-KOH (pH 7.2), 500 mM NaCl, 1 mM DTT, and 50% glycerol. The yield of the purified enzyme from 1 L of cell culture is ~2 mg. The purity is estimated to be greater than 95% as judged by SDS−polyacrylamide gel electrophoresis.

Preparation of tRNA Substrates. Duplex DNA templates for in vitro transcription of *E. coli* tRNA^{Gln} (CUG) and *M. thermautotrophicum* tRNA^{Gln} (CUG) were synthesized from two single-stranded oligodeoxynucleotides containing a complementary overlap duplex region, as described previously (*24*). For the *M. thermautotrophicum* tRNA, the oligonucleotides used were 5′ AATTCCTGCAGTAATACGACTCACTATAAGTCCCGTGGGGTAATGGCAATCCTGAT and 5′ mUmGGTAGTCCCGAGCGGAGTCGAACCGCTATCGATGGATCCAGAGTCCATCAGGATTG, where the underlined region represents the T7 RNA polymerase promoter sequence. For both tRNAs, the two 3′-terminal deoxynucleotides on the noncoding strand incorporated 2′-*O*-methyl sugars (mU and mG in the sequences), to improve the fidelity of transcription termination by T7 RNA polymerase. This thereby generates a high proportion of enzymatically active tRNA transcripts. The *E. coli* tRNA^{Gln} gene was synthesized with a catalytically neutral U1G mutation to promote efficient transcription initiation (*24*).

Milligram quantities of each tRNA were transcribed with the Del(172−173) variant of T7 RNA polymerase, as described previously (*24*, *25*); we found that the presence of A1 in *M. thermautotrophicus* tRNA^{Gln} reduced yields by only 2-fold.

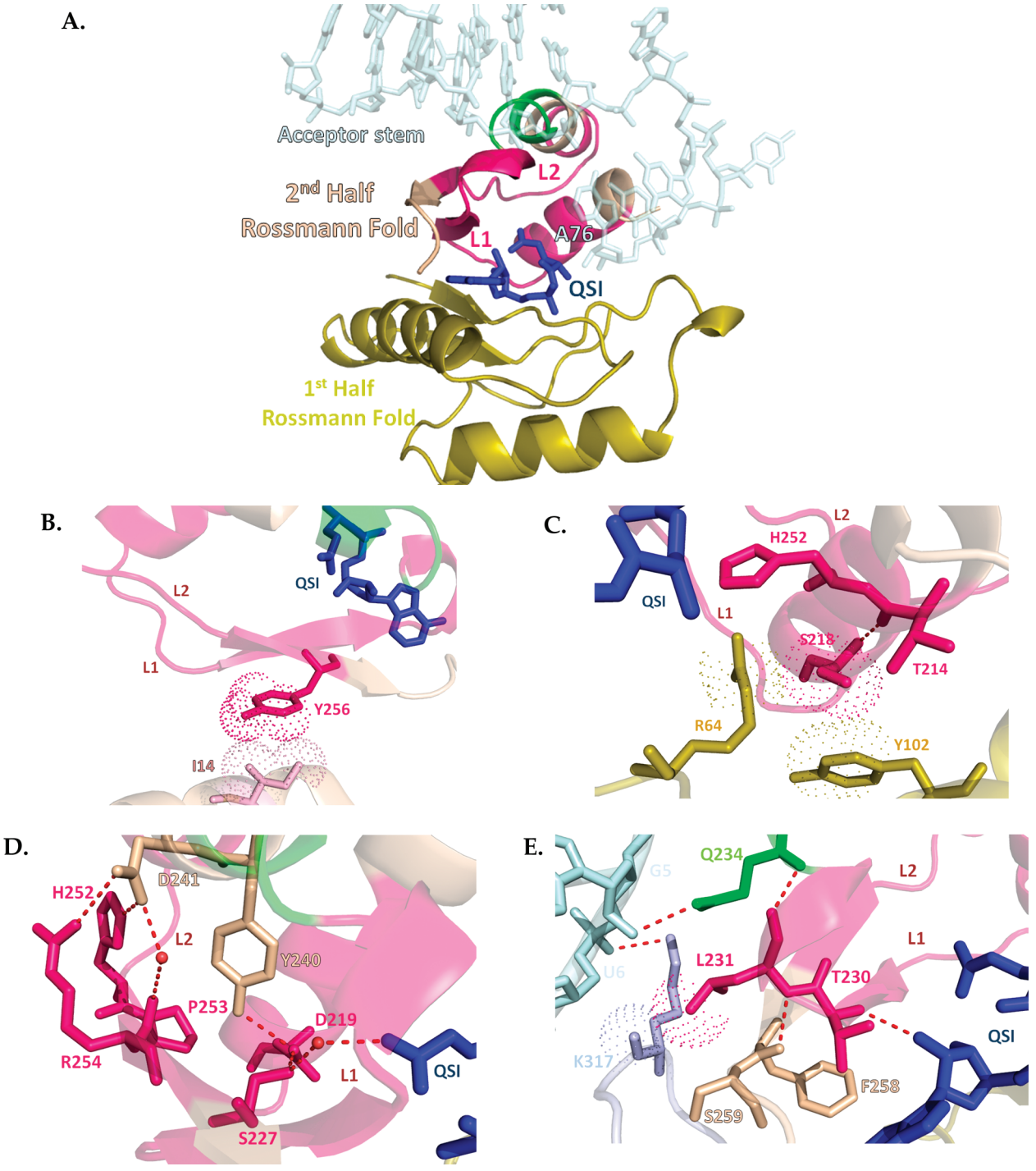

FIGURE 1: (A) Active site Rossmann fold domain structure of wild-type *E. coli* GlnRS bound in a ternary complex with $tRNA^{Gln}$ and the glutaminyl adenylate analogue 5′-*O*-[*N*-(L-glutaminyl)sulfamoyl]adenosine (QSI) (*41*). L1 and L2 designate loops that bridge secondary structure elements in the second half of the fold and that were replaced in the engineered enzymes. The α-helical segment colored green contains amino acids that directly bind the acceptor stem of the tRNA; these residues were not exchanged in the hybrids. The portion of the protein structure that was introduced from human GluRS, to produce the hybrid enzyme GlnRS S1/L1/L2, is colored pink. (B) Location of GlnRS Tyr256 in the final *β*-strand of the second half of the Rossmann fold, with respect to the active site (shown by the binding of QSI). van der Waals interactions of Tyr256 with Ile14 from the N-terminal helical peptide of GlnRS (which precedes the first half of the Rossmann fold) are depicted. (C) Location of GlnRS Ser218 in the first α-helix of the second half of the Rossmann fold. van der Waals interactions with Arg64 (first half of the Rossmann fold) and Tyr102 (located in the peptide immediately following the first half of the fold) are shown. Arg64 is conserved in human GluRS, and Tyr102 is substituted with histidine in that enzyme. (D) Interactions of GlnRS Tyr240 and Asp241 with surrounding residues in the second half of the Rossmann fold. Hydrogen bonds are depicted by dotted pink lines. All residues colored pink were replaced in the hybrid enzymes. QSI marks the position of the active site at the bottom right. (E) Interactions of GlnRS Leu231 with its surrounding environment in the RNP complex. Hydrogen bonds are depicted as dotted pink lines. Both Gln234 and Lys317 directly interact with the tRNA backbone. Interaction of the adjacent Thr230 with the sugar of QSI, an interaction preserved in the structure of the RNP bound to ATP (*6*), is also shown. The tRNA acceptor stem is colored light blue at the top left.

For each tRNA, the transcription reaction mixtures were loaded on 5 mL DE-52 (Whatman) columns, eluted, precipitated with ethanol, dried, and stored either dried (*E. coli* $tRNA^{Gln}$) or in 10 mM Tris (pH 8.0) and 1 mM EDTA (*M. thermautotrophicum*

Table 1: Kinetic Properties of Hybrid GlnRS Enzymes

enzyme	K_m(Glu) (mM)	k_{cat}(Glu)[a] (s^{-1})	k_{cat}/K_m(Glu) (M^{-1} s^{-1})	K_m(ATP) (mM)	k_{cat}(ATP)[a] (s^{-1})	k_{cat}/K_m(ATP) (M^{-1} s^{-1})	K_m(tRNA^{Gln}) (μM)	k_{cat}(tRNA^{Gln})[a] (s^{-1})	k_{cat}/K_m(tRNA^{Gln}) (M^{-1} s^{-1})
WT GlnRS	> 750[b]	0.046 ± 0.013[b]	(9.5 ± 1.3) × 10^{-4}[c]	0.21[d]	–	–	0.31 ± 0.09[e]	3.2 ± 0.5[e]	1.0 × 10^{7}[e]
L1L2	5.8 ± 0.5[f]	0.09 ± 0.02[f]	15.5[f] [16300]	0.62 ± 0.01	0.1 ± 0.01	160	7.6 ± 3.0	0.04 ± 0.01	5.2 × 10^{3}
V218S	8.9 ± 1.0	0.06 ± 0.01	6.7 [7000]	ND	–	–	4.5 ± 0.6	0.04 ± 0.005	8.8 × 10^{3}
W256Y	2.6 ± 1.0	0.1 ± 0.04	38.5 [40500]	ND	–	–	4.8 ± 0.2	0.14 ± 0.01	2.9 × 10^{4}
T231L	21.2 ± 1.2	0.09 ± 0.01	4.2 [4400]	ND	–	–	8.05 ± 0.45	0.08 ± 0.01	9.9 × 10^{3}
Y240D/D241F	21.1 ± 1.1	0.09 ± 0.01	4.3 [4500]	ND	–	–	5.3 ± 0.3	0.04 ± 0.01	7.5 × 10^{3}

[a] k_{cat} values represent lower bounds and assume that the enzyme preparations are fully active (see Experimental Procedures). [b] The K_m for glutamate in glutamylation by WT GlnRS could not be determined, because saturation is not observed. k_{cat} was determined from reactions in which the concentration of tRNA^{Gln} was varied at 10 mM ATP and 1.0 M glutamate (*16*). [c] k_{cat}/K_m is derived from the linear slope of a *V* vs Glu concentration plot in which saturation for Glu is not observed (*21*). [d] This value was previously reported (*30*). [e] These parameters represent values for cognate Gln-tRNA^{Gln} synthesis reactions (*40*). [f] These values were previously reported (*26*). The numeral in brackets represents the fold improvement compared with that of WT GlnRS.

Table 2: Kinetic Analysis of *M. thermoautotrophicus* GluRSND

	tRNA^{Gln}		Glu		ATP	
k_{max} (s^{-1})	k_{cat} (s^{-1})[a]	K_m (nM)	k_{cat} (s^{-1})[a]	K_m (mM)	k_{cat} (s^{-1})[a]	K_m (mM)
0.12 ± 0.01	0.10 ± 0.01	38 ± 10	0.09 ± 0.05	6.2 ± 0.6	0.10 ± 0.05	3.1 ± 1.7

[a] k_{cat} values represent lower bounds and assume that the enzyme preparations are fully active (see Experimental Procedures).

tRNA^{Gln}) at −20 °C. Prior to use, the tRNAs were resuspended in highly purified water or in 10 mM Tris and 1 mM EDTA.

Enzyme Kinetics. The aminoacylation assays were performed using *E. coli* or *M. thermautotrophicum* tRNA^{Gln} transcripts ^{32}P-labeled at the 3′-terminal internucleotide linkage using the exchange reaction of tRNA nucleotidyltransferase, as described previously (*19*, *21*, *26*). For *E. coli* tRNA^{Gln}, labeled tRNA was purified on a Bio-Rad P30 spin column and then mixed with unlabeled tRNA to the desired final concentration. The tRNA was then refolded by incubation at 80 °C for 2−3 min, followed by addition of $MgCl_2$ to a final concentration of 10 mM, and slow-cooling to ambient temperature over a period of 15−30 min. For *M. thermautotrophicum* tRNA^{Gln}, labeled tRNA was also purified on a Bio-Rad P30 spin column but was then further purified on a 20% native polyacrylamide gel prior to mixing with unlabeled tRNA and refolding as described above. All steady-state aminoacylation reactions were quenched by the addition of 400 mM sodium acetate (pH 5.2). Single-turnover reactions performed for the *M. thermautotrophicum* GluRSND were conducted using a Kintek RQF-3 rapid chemical-quench kinetics apparatus and were quenched in a solution containing 400 mM sodium acetate (pH 5.2) and 0.1% SDS. P1 nuclease digestions were performed by addition of 1−5 μL of the quenched reaction mixture to a microtiter well containing 3−5 μL of 0.01−0.1 mg/mL P1 nuclease (Fluka) in quenching buffer. After incubation for 8−10 min, the reaction mixtures were spotted on prewashed PEI-cellulose TLC plates (Sigma) and developed in 100 mM ammonium acetate and 5% (v/v) acetic acid. Dried TLC plates were quantitated by phosphorimaging analysis. Single-turnover reactions were fit to a single-exponential function to derive k_{obs}. Initial velocities in multiple-turnover reactions were fit to the Michaelis−Menten equation and analyzed with Eadie−Hofstee plots.

For *M. thermautotrophicum* GluRSND, reactions were conducted at 37 °C in 50−100 mM Hepes-KOH (pH 7.0), 10 mM $MgCl_2$, and 5 mM DTT, unless otherwise noted. For the hybrid enzymes derived from *E. coli* GlnRS, reactions were performed at 37 °C in 50 mM Tris (pH 7.4), 10 mM $MgCl_2$, and 5 mM DTT. The concentrations of enzymes and substrates used in each experiment are provided together with the results given below. For both the hybrid enzymes and *M. thermautotrophicum* GluRSND, active site titrations were not performed because burst kinetics at the aminoacylation step were not indicated, and because the product release-limited adenylate formation reaction cannot be performed in the absence of tRNA. The reported k_{cat} values assume that the enzyme preparations are fully active and thus represent lower bounds (Tables 1 and 2).

RESULTS

Amino Acid Complementarity in Hybrid GlnRS Enzymes Synthesizing Glu-tRNA^{Gln}. Our previous work has demonstrated that amino acid specificity is a distributed property of the GlxRS Rossmann fold domain (*20*). The WT *E. coli* GlnRS enzyme, which serves as the target platform for the protein engineering experiments, exhibits 10^7-fold specificity for glutamine over glutamate, as measured by k_{cat}/K_m with respect to the amino acid (k_{cat}/K_m[AA]), for synthesis of Gln-tRNA^{Gln} versus the misacylated Glu-tRNA^{Gln} (*21*). Replacement of Cys229, Gln255, Ser227, and Phe233 in the primary glutamine binding site of *E. coli* GlnRS, with their equivalents in the evolutionarily related β-class human GluRS, improves k_{cat}/K_m for Glu-tRNA^{Gln} synthesis by just 20-fold. The very high K_m of 230 mM for glutamate in this quadruply mutated enzyme further underscores that the local environment of the amino acid binding pocket functions in synergy with more distal regions to generate selectivity against glutamate. Further replacement of the L1 loop from human GluRS (amino acids Thr214−Leu231 in *E. coli* GlnRS) reduces K_m[Glu] to 44 mM, while replacement of the L2 loop as well (amino acids Val243−Tyr256 in *E. coli* GlnRS) reduces K_m[Glu] to 5.8 mM (*20*). The k_{cat} of this hybrid enzyme (GlnRS S1/L1/L2) is measured at 0.09 s^{-1}, ∼35-fold lower than the k_{cat} of WT GlnRS for Gln-tRNA^{Gln} synthesis. On the basis of comparison with WT GlnRS, the hybrid remains 800-fold reduced in k_{cat}/K_m[AA] for aminoacyl-tRNA synthesis. GlnRS S1/L1/L2 is constructed from 22 amino acid substitutions and one deletion in WT GlnRS and is completely inactive in cognate Gln-tRNA^{Gln} synthesis (ref *20* and Figure 1A). This hybrid

enzyme represents a significant achievement in the reengineering of amino acid specificity in a tRNA synthetase.

All of the replaced amino acids in GlnRS S1/L1/L2 are from the second half of the catalytic Rossmann fold, which in total comprises amino acids 211−260 of the enzyme. Inspection of the cocrystal structure shows that the replaced portion of GlnRS constitutes a fairly compact subdomain that extends to solvent at the surface opposite the active site cleft and makes interactions with surrounding protein structure at a number of positions (Figure 1A). Although there is some conservation of sequence between GlnRS and GluRS at these interfaces, at many positions non-native contacts must occur between introduced GluRS amino acids and the surrounding GlnRS structure. We thus systematically examined these regions with a view toward identifying whether any of the new interactions might disrupt the protein structure on electrostatic or steric grounds. We reasoned that correcting such unfavorable contacts by further mutagenesis could unmask a more efficient Glu-tRNA^{Gln} synthesis activity.

Two positions were identified in this manner. First, GlnRS Tyr256 within loop L2 is a partially solvent-accessible residue that also packs on Ile14 from the short, partly helical N-terminal peptide (residues 1−25) that precedes the first half of the Rossmann fold (Figure 1B). In GlnRS S1/L1/L2, Tyr256 is substituted with tryptophan. The bulkier indole side chain at Trp256 in the hybrid could clearly disrupt packing with the N-terminal segment. Second, the hydroxyl group of GlnRS Ser218 within loop L1 donates a hydrogen bond to the backbone amide at position Thr214 within L1 and also packs on residues Arg64 from the first half of the Rossmann fold (residues 26−99) and Tyr102 from the inserted domain (residues 100−210) (Figure 1C). In GlnRS S1/L1/L2, Ser218 is substituted with valine. Again, removal of an internal hydrogen bond together with potential steric clashes with surrounding protein could disrupt the structure. Accordingly, to restore the native interactions, we conducted site-directed mutagenesis using the GlnRS S1/L1/L2 gene as a template, to separately revert Trp256 of GlnRS S1/L1/L2 to tyrosine (W256Y) and Val218 of GlnRS S1/L1/L2 to serine (V218S). The enzymes were targeted to the periplasm for expression, as described for the parent hybrid (*20*). Steady-state kinetic analysis of the two new enzymes was conducted with 250 or 500 nM enzyme at 10 mM ATP and 30 μM tRNA^{Gln}, while the concentration of glutamate was varied between 0.1 and 30 mM. The catalytic efficiency of V218S is decreased by 3-fold compared with that of GlnRS S1/L1/L2, with the effects divided roughly equally between k_{cat} and K_m. However, in W256Y, K_m[Glu] is decreased 2-fold while k_{cat} remains unchanged (Table 1 and Figure 2). Thus, each of these third-shell packing interactions, found at an interface between *E. coli* GlnRS and human GluRS sequences, exerts a modest influence on the efficiency of the enzyme. The lower K_m[Glu] in W256Y reflects an improved hybrid enzyme design; this mutant possesses k_{cat}/K_m[AA] that is reduced 260-fold compared with that of WT GlnRS.

In addition to unmasking an inherent catalytic efficiency by correcting distal packing defects, we also considered whether further, thus-far unconsidered substitutions adjacent to the amino acid pocket might also improve activity. The capacity for further improvement was suggested by the lower amino acid K_m values (100−200 μM) that have been reported for members of the GlxRS enzyme family (*19*, *27*, *28*). While nearly all of the amino acids in and around the GlnRS amino acid binding pocket have already been substituted in GlnRS S1/L1/L2, a prominent exception is Tyr240, a third-shell residue that donates a hydrogen bond from its phenolic hydroxyl group to the side chain carboxylate of Asp219. Asp219, in turn, is connected via a water-mediated hydrogen bonding network to substrate glutamine (Figure 1D). In the context of WT GlnRS, mutations of Tyr240 to glutamate or glycine decreased K_m for glutamine by 2−3-fold, with no effect on k_{cat}/K_m for aminoacylation (*29*). The adjacent amino acid, Asp241 of *E. coli* GlnRS, was also not substituted in the construction of GlnRS S1/L1/L2. Its side chain carboxylate group accepts hydrogen bonds from the imidazole and guanidinium moieties of His252 and Arg254, respectively,

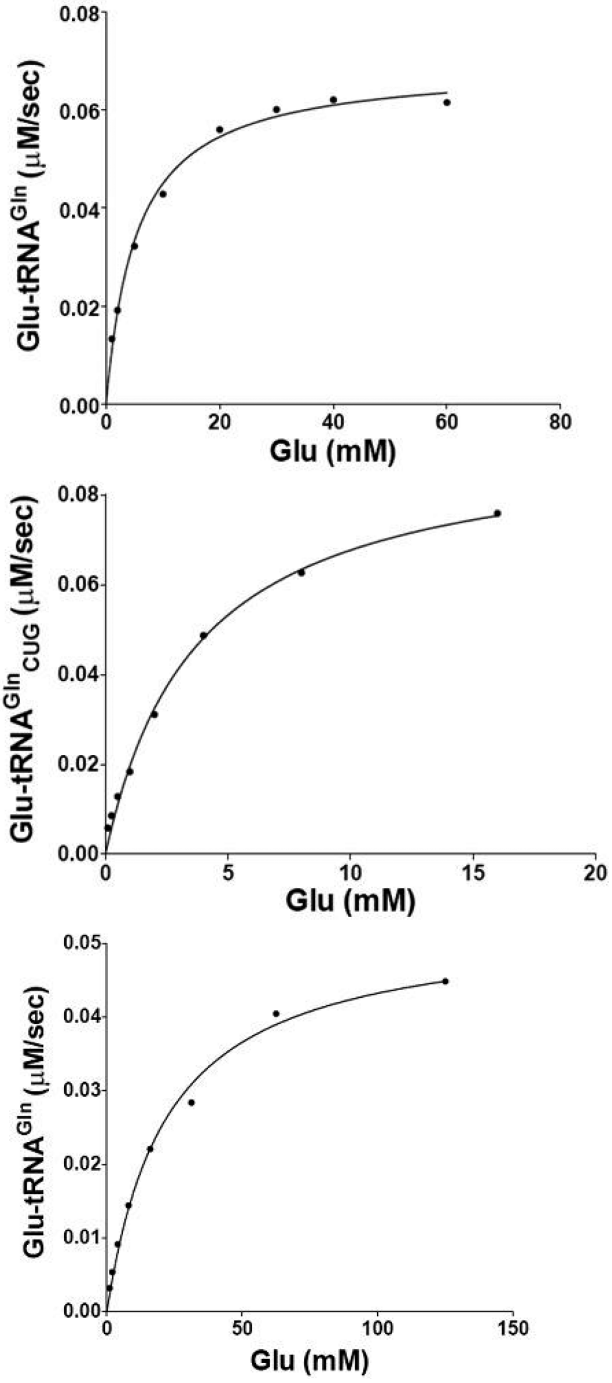

FIGURE 2: Plots of initial velocity vs substrate concentration used for determination of K_m[Glu] in GlnRS S1/L1/L2 (top), W256Y (middle), and Y240D/D241F (bottom). In each case, the data were fit to the Michaelis−Menten equation.

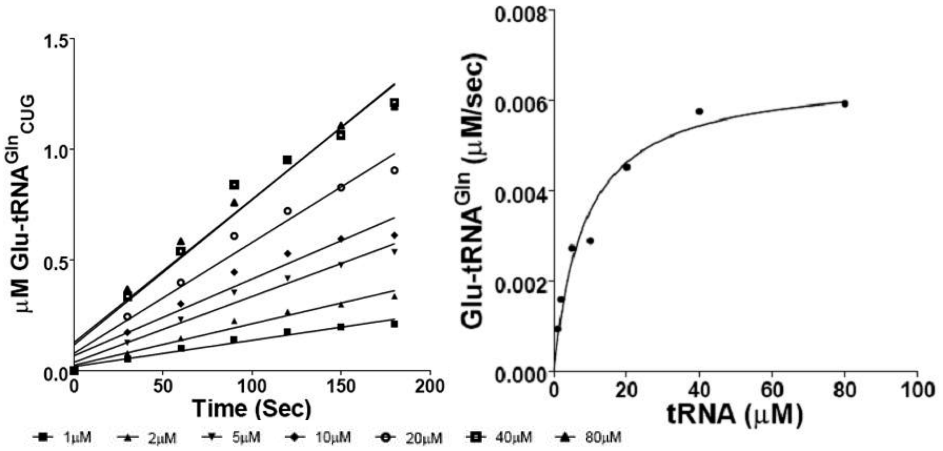

FIGURE 3: Initial velocities (left) for determination of steady-state kinetic parameters for the T231L hybrid enzyme, with respect to tRNA concentration (listed at the bottom) and replot (right) of the initial velocity data to yield k_{cat} and K_m[tRNA].

within loop L2. Inclusion of Tyr240 and Asp241 in the hybrid enzyme design, then, would appear to have the capacity to influence the detailed structure and/or dynamics of the glutamate binding pocket, with possible effects on catalytic function.

Substitution of Tyr240 and Asp241 with their equivalents in human GluRS (Phe and Tyr, respectively) was conducted by site-directed mutagenesis using the GlnRS S1/L1/L2 gene as a template, and the new hybrid enzyme (Y240F/D241Y) containing 25 substitutions toward human GluRS was expressed and purified to homogeneity. Steady-state kinetics with respect to glutamate was determined at 250 nM enzyme, 10 mM ATP, and 30 μM tRNA^{Gln}, with concentrations of glutamate in the range of 1−150 mM. Although we anticipated that these additional substitutions might improve performance, we found instead that K_m[Glu] is increased 4-fold while k_{cat} remains unchanged (Table 1). Because both k_{cat} and complementarity for tRNA (see below) are maintained in Y240F/D241Y, it appears most likely that the decreased complementarity for glutamate arises from a more local disruption in the structure or dynamics of the binding pocket. However, all of the interactions thought to be made by Phe240 are with residues imported from human GluRS (Figure 1C), while Tyr241 occupies a solvent-accessible position at which it also appears to be easily accommodated. The 4-fold decrease in k_{cat}/K_m by Y240F/D241Y may then reflect dynamic interactions either with more distal regions of the protein that are retained as GlnRS sequences or with the nearby acceptor stem of the tRNA.

Relationship between tRNA and Amino Acid Binding Sites in the Hybrid Enzymes. The 16000-fold enhancement of k_{cat}/K_m for Glu-tRNA^{Gln} synthesis by GlnRS S1/L1/L2 represents an evaluation with respect to the binding of the amino acid. A full assessment of function must also examine the efficiency with which the hybrid interacts with ATP and tRNA^{Gln}. To address this, we first measured K_m for ATP in the aminoacylation reaction at 250 nM enzyme, 30 μM tRNA^{Gln}, and 100 mM glutamate, using ATP concentrations ranging from 0.1 to 16 mM. The K_m value is 620 ± 10 μM, which is elevated by only 3-fold compared with that of WT GlnRS [K_m of WT GlnRS for ATP is 210 μM (*30*) (Table 1)]. Thus, it appears that the integrity of the ATP binding site in GlnRS S1/L1/L2 is largely preserved. Although we have not measured K_m[ATP] for the other hybrids, the relatively similar values obtained for k_{cat} and K_m[Glu] suggest that the ATP binding site remains intact in these enzymes as well.

We next measured K_m[tRNA] for GlnRS S1/L1/L2 and for its Y240F/D241Y, W256Y, and V218S derivatives, at 100 nM (Y240F/D241Y, W256Y, and V218S) or 250 nM (GlnRS S1/L1/L2) enzyme, saturating levels of glutamate (200 mM) and ATP (10 mM), and tRNA concentrations ranging from 1 to 80 μM (Y240F/D241Y, W256Y, and V218S) or from 2 to 80 μM (GlnRS S1/L1/L2). In all four hybrids, K_m[tRNA] is elevated by 15−30-fold, as compared with the value of 0.3 μM measured in the cognate GlnRS reaction (Table 1). These findings demonstrate that the engineered specificity for glutamate has been achieved at significant cost to the complementarity of the enzyme−tRNA interface. The new data provide additional support for the notion that the amino acid and tRNA binding sites in GlnRS are interdependent (*16*, *20*).

The elevated tRNA K_m value in GlnRS S1/L1/L2 prompted us to reexamine its sequence with a view toward elucidating whether any of the introduced residues might function to directly couple the amino acid and tRNA binding sites. Five consecutive α-helical residues, located at positions 234−238 in the second half of the GlnRS Rossmann fold, each make either direct or water-mediated interactions with the tRNA acceptor stem (Figure 1A). None of these residues were substituted in GlnRS S1/L1/L2, because the aim of the design was to test the extent to which the amino acid and tRNA selectivities can be separated in GlxRS enzymes (*20*). However, a short loop preceding these amino acids, at positions Thr230−Phe233, makes diverse interactions. Among these four residues, Thr230 and Glu232 are conserved in human GluRS and have roles in ATP binding, while Phe233 was substituted (with tyrosine) because it forms part of the amino acid pocket. The role of the partly solvent accessible Leu231, which was converted to Thr in GlnRS S1/L1/L2, has been unclear. In WT GlnRS, Leu231 contacts main chain and side chain atoms of Gln234, Phe258, Ser259, and Lys317 and approaches to 4.3−4.5 Å of the 2′-OH ribose moiety of C5 in the tRNA acceptor stem (Figure 1E). Therefore, while Leu231 does not directly contact tRNA, it may stabilize the direct tRNA interactions made by Gln234 and Lys317. Further, the equivalent residue in *T. thermophilus* GluRS, Glu207, directly accepts a hydrogen bond from the 2′-OH moiety at C5 of tRNA^{Glu} (*31*). It appears then that the amino acid at Rossmann fold position 231 could provide tRNA complementarity or could link the amino acid and tRNA binding sites in the hybrid enzymes.

To isolate the amino acid selectivity function of the protein portion of the GlxRS RNP as clearly as possible, we thus

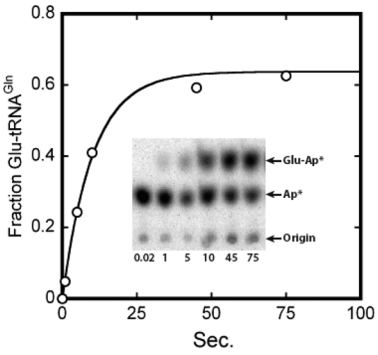

FIGURE 4: Time course for Glu-tRNA^{Gln} formation by *M. thermautotrophicus* GluRSND. In this experiment, the enzyme concentration is 500 nM, and 3′-^{32}P-labeled tRNA is present at a final concentration of <1 nM. This represents saturation for tRNA binding. The inset shows a TLC plate demonstrating the separation of substrate (Ap*; center of TLC plate) and product (Glu-Ap*; top of TLC plate). The reaction mixtures were spotted at the bottom of the plate. The ratio of intensities for Glu-Ap* and Ap* yields the plateau aminoacylation value.

generated a new GlnRS S1/L1/L2 hybrid containing the T231L reversion and analyzed its steady-state kinetic properties with respect to glutamate and tRNA^{Gln}, using enzyme and tRNA levels identical to those of the other hybrids. We find that k_{cat} and K_m[tRNA] are unchanged but that K_m[Glu] is elevated by 4-fold compared with that of GlnRS S1/L1/L2 (Table 1). Thus, including the Leu231 substitution in the original design improves complementarity for glutamate, even though the position of this residue implies a more direct role in tRNA binding. It appears then that the short bridging peptide at positions 230−233 plays a critical role in bridging all three substrate binding sites (Figure 3).

Benchmarking the Activities of the Hybrid Enzymes. An important benchmark for the efficiency of the reconstructed enzymes is comparison with a naturally occurring enzyme that catalyzes Glu-tRNA^{Gln} synthesis. For these measurements, we chose the evolutionarily related *M. thermautotrophicum* GluRSND, which possesses the β-type anticodon binding domain found in *E. coli* GlnRS. This enzyme has been previously expressed in *E. coli* (*23*), and a structure of the apoenzyme refined at 1.65 Å resolution has recently been reported (*12*). We purified the recombinant enzyme from *E. coli* to homogeneity using the previously reported expression construct. tRNA^{Gln}-(CUG) from *M. thermautotrophicum* was generated as a T7 RNA polymerase in vitro transcript without mutation of the A1 residue, since high levels of RNA were produced despite the absence of 5′G in the construct (see Experimental Procedures). After refolding, 3′-end labeling, and gel purification of the tRNA, we first tested aminoacylation capacity using single-turnover kinetics with 2 nM to 2 μM GluRSND and <1 nM labeled tRNA^{Gln}, at 10 mM ATP and 50 mM glutamate (Figure 4). At saturating enzyme levels ($\geq$250 nM), the observed rate k_{obs} reaches a maximum of 0.12 s^{-1} (k_{max}) (Table 2). This value represents either the rate of the chemical steps on the enzyme or that of a closely linked first-order rearrangement of the complex before initiation of the bond-breaking and bond-making steps. Plateau aminoacylation levels were consistently in the range of 60−75% for all the experiments reported here (Figure 4).

We next determined K_m(ATP), K_m(Glu), and K_m(tRNA^{Gln}) under multiple-turnover conditions. K_m[ATP] and K_m[Glu] were measured using 500 nM tRNA^{Gln} and 10 nM GluRSND, with constant levels of 50 mM glutamate and 10 mM ATP in reaction mixtures where the concentrations of ATP and glutamate, respectively, were varied. K_m[tRNA] was measured using 2 nM GluRSND, 10 mM ATP, 50 mM glutamate, and 0.02−1.0 μM tRNA. The k_{cat} values determined in these three experiments are identical within experimental error, providing an internal check on the precision of the measurements (Table 2). The value of k_{cat} is also very similar to the single-turnover k_{max}, indicating that the rate-limiting step corresponds to the first-order conformational rearrangement, or to the chemical steps. K_m[tRNA] is relatively low compared with those of other tRNA synthetases, suggesting good complementarity at the enzyme−tRNA interface. This also suggests that post-transcriptional modification is unlikely to be important to aminoacylation, consistent with the presence of C34 rather than U34 in the 5′-anticodon position. Although the importance of U34 modification to glutamylation in archaea is not known, 2-thiolation of U34 in bacterial tRNA^{Glu} lowers K_m[tRNA] for glutamylation (*32*, *33*).

The K_m values determined for ATP and glutamate are higher than those typically found for tRNA synthetases (Table 2). The value for K_m[ATP] is approximately 15-fold higher than that determined for *E. coli* GlnRS (*30*) or *E. coli* GluRS^{D} (*28*) (Table 2). A millimolar K_m for ATP has also been reported for *M. thermautotrophicum* pyruvate carboxylase, suggesting compatibility with physiological function in this organism (*34*). The K_m[Glu], similarly, is 60-fold higher than the value of 100 μM reported for *E. coli* GluRS^{D} (*28*). This may reflect the physiology of the thermophilic methanogen, or a particular feature of misacylating reactions generally. No determination of K_m[ATP] or K_m[Glu] for a Glu-tRNA^{Gln} synthesis reaction has previously been reported. To evaluate whether the unusually high K_m values might be related to the discrepancy between the temperature of 37 °C at which the assays are performed and the temperature optimum for the organism of 65 °C, we also measured initial velocities at 52 °C, at which the tRNA^{Gln} transcript remains folded. As expected, k_{cat} for Glu-tRNA^{Gln} synthesis increased approximately 4-fold at this elevated temperature, but K_m[ATP] and K_m[Glu] were unchanged (data not shown).

Recently, k_{cat} and K_m[tRNA] for Glu-tRNA^{Gln} synthesis at 37 °C by *M. thermautotrophicum* GluRSND were reported by another laboratory (*35*). The values determined (k_{cat} = 0.7 min^{-1}, and K_m[tRNA^{Gln}] = 2.1 μM) are 10-fold lower and 55-fold higher, respectively, than the values we have measured (Table 2), suggesting a much more weakly functioning enzyme. However, we anticipate that these values reflect the subsaturating level of glutamate (1 mM) and the elevated concentration of enzyme (50 nM) that were used in the experiments. It was also reported that tRNA^{Gln} binds GluRSND with a K_d of 37 nM, a value that is identical to the K_m[tRNA] that we have measured (Table 2). A finding of identical values for K_m and K_d is consistent with a rate-determining step that follows substrate binding but precedes product release, as we have independently demonstrated here by the equivalence of k_{cat} and k_{max} in the multiple-turnover and single-turnover experiments, respectively (Table 2). No explanation for the large reported discrepancy between K_m[tRNA] and K_d[tRNA] was offered in the previous work. Measurements of k_{max}, K_m[ATP], and K_m[Glu] were not reported (*35*).

DISCUSSION

Coevolution of tRNA and tRNA Synthetase Sequences. We have demonstrated that engineered *E. coli* GlnRS-derived hybrid enzymes catalyze Glu-tRNA^{Gln} synthesis with efficiencies

comparable to that of a naturally occurring enzyme, the *M. thermautotrophicum* GluRSND. Both enzymes exhibit k_{cat} values of approximately 0.1 s^{-1}, while K_m[Glu] in the W256Y revertant is 2-fold lower than in the naturally occurring enzyme. However, the naturally occurring and engineered enzymes diverge markedly in their respective capacities to provide a binding interface for tRNA^{Gln}: K_m[tRNA] for the methanogen-derived enzyme is 200-fold lower than in the hybrids (Tables 1 and 2).

These findings provide evidence that the tRNA and amino acid selection functions in these tRNA synthetases do not operate independently. With the possible exception of Thr231, none of the 23 replaced amino acids in GlnRS S1/L1/L2 interact with tRNA (Figure 1A,E). Accordingly, if the binding sites for amino acid and tRNA functioned independently, it would be expected that K_m[tRNA] would more closely match that of the parent WT *E. coli* GlnRS. That it does not is a clear demonstration that the GlnRS protein architecture has differentiated to provide a matching function: the tRNA^{Gln} binding site is not properly configured in the absence of cognate glutamine, even though an apparently well-formed glutamate binding site replaces the WT glutamine pocket. The occurrence of enzyme homologues such as the β-class GlnRS/GluRSND pair, which differ in amino acid specificity in the context of the same tRNA isoacceptor specificity, demonstrates that across evolutionary time the common Rossmann fold protein scaffold has the capacity to differentiate in such a way as to match either glutamate or glutamine with tRNA^{Gln}. The very high K_m[tRNA] values of the engineered hybrids show that this matching function has not been reproduced in the engineered enzymes.

The notion that tRNA synthetase and tRNA sequences have coevolved suggests a process of optimization by which acquired mutations in either macromolecule improve catalytic efficiency for cognate but not noncognate amino acid pairing. This coevolution occurs within the context of a particular amino acid specificity (*15*, *36*). The implication is that certain tRNA nucleotides function together with key residues in the enzyme, to optimize the formation of a selective amino acid pocket. If this general conceptual framework is correct, then optimizing the Glu-tRNA^{Gln} synthesis activity of the engineered hybrids will very likely require alteration of the enzyme−tRNA interface. Successful nucleotide alterations are predicted to be those that collaborate with the enzyme to optimize the tRNA−amino acid pairing. Such nucleotides might be considered as an embedded signature in the tRNA: a second identity set that functions not to select tRNA^{Gln} from the cellular tRNA pool but, instead, to assist the enzyme in forming a selective glutamate binding site. The tRNA requirement for aminoacyl adenylate synthesis gives this notion added force in the GlxRS family and in class I ArgRS and LysRS, but we suggest that tRNA collaboration in amino acid selection may be a feature of other tRNA synthetases as well. The protein engineering approach we are pursuing represents an in-depth attempt to delineate which distinct elements of homologous tRNA synthetase architectures are responsible for divergent RNA−amino acid pairing specificities. The work presented here provides crucial validation of the experimental system by clearly demonstrating which properties of naturally occurring enzymes have been recapitulated and which have not, and by demonstrating robust catalytic function in five different hybrids.

It is remarkable that the engineered hybrids match and indeed surpass the K_m[Glu] of *M. thermautotrophicum* GluRSND, and this finding can perhaps be taken to indicate a successful design for amino acid binding. Thus, complementarity for the amino acid perhaps could be viewed as a property of the protein alone, and not as a joint property of the RNP. However, it is premature to take this comparison as definitive. Arguably, *M. thermautotrophicum* GluRSND, a β-class GluRS capable of Glu-tRNA^{Gln} synthesis, is indeed a better model for the GlnRS hybrids than *E. coli* α-GluRS^{D}, for which K_m[Glu] is reported to be 100 μM (*28*). The latter enzyme possesses a structurally distinct anticodon-binding domain and pairs glutamate with tRNA^{Glu} instead of tRNA^{Gln}. However, it should be noted that there is no known naturally occurring β-class GluRS that is a specific misacylator that does not also retain the capacity to form Glu-tRNA^{Glu}. Possibly, the bacterial α-class GluRS2 enzymes, which may solely form Glu-tRNA^{Gln}, may be better models even though they diverge further from GlnRS (*14*, *15*). Alternatively, since the gene duplication leading to GlnRS occurred after differentiation of the eukarya, a β-class eukaryotic GluRS^{D} might also offer a relevant comparison. These considerations highlight the need for a systematic and rigorous examination of the kinetic properties of representatives of all six GlxRS subclasses: GlnRS, α-GluRS^{D}, β-GluRS^{D}, α-GluRSND, β-GluRSND, and GluRS2. Most of this information remains unavailable; for example, to the best of our knowledge, the K_m[Glu] has only previously been reported for the relatively well-studied *E. coli* GluRS^{D} and for the α-class *Mycobacterium tuberculosis* GluRSND (*28*, *37*).

Design of E. coli GlnRS-Derived Enzymes That Synthesize Glu-tRNA^{Gln}. We have explored the functional characteristics of GlnRS S1/L1/L2 by measuring a full set of steady-state kinetic parameters and by using further site-directed mutagenesis to assess the efficacy of the design. As we have noted, the still-narrow initial question has been to ask whether the amino acid selection function of GlnRS could be exchanged with that of a GluRS, by manipulating just the protein portion of the RNP. We have now shown that K_m[Glu] for the hybrids matches that of a naturally occurring GluRS enzyme, but the values measured in the millimolar range are unexpectedly high (Tables 1 and 2). A minimum answer to the query would then be that a functional glutamate binding site has indeed been created, and that some further optimization may yet be possible.

The four new hybrid enzymes possess steady-state kinetic characteristics that are not markedly different from the original design: at most, 4-fold changes in K_m(AA) for amino acid are measured, and the K_m[tRNA] values vary less than 2-fold (Table 1). The modest kinetic effects measured for V218S and W256Y suggest that there is not a great deal of structural incompatibility at the interfaces between the human GluRS and *E. coli* GlnRS portions of the enzymes. No other positions along the interfaces between the GluRS and GlnRS sequences appear to create unfavorable steric or electrostatic appositions. Thus, we tentatively conclude that the inserted GluRS substructure in GlnRS S1/L1/L2 contributes to a stable Rossmann fold in the hybrid enzymes.

Our findings do not yet establish a minimal component of protein structure that could suffice to bring about the amino acid specificity change that we have demonstrated. We have shown that replacement of four amino acids in the S1 site alone reduces K_m[Glu] of WT GlnRS to just 230 mM, and that the addition of loop L1 to the design produces a hybrid possessing a K_m[Glu] that remains 10-fold above that of GlnRS S1/L1/L2 (*20*). We anticipate that careful structure-based analysis could lead to the design of mutants that bring about the functional change with substantially fewer than the 23 amino acid replacements we have constructed. Pursuit of this important question, which should

provide detailed insight into the importance of distal structural elements in conferring substrate selectivity, remains open as a topic for future research. It is also possible that additional substitutions in the protein, in the third and fourth shells surrounding the amino acid pocket, could precipitate further improvement of catalytic parameters. For example, reverting Val218 to Ser in V218S did not improve catalytic efficiency, suggesting that the introduction of Val218 did not create an unfavorable steric clash with surrounding GlnRS residues. However, Ser218 interacts with Tyr102 of GlnRS, a position occupied by histidine in human GluRS (Figure 1C). Possibly, then, introducing Y102H could improve the design. Many such experiments can be envisioned. Intuitively, however, it seems unlikely that further mutagenesis of distal protein residues would be likely to lower K_m[tRNA], the major functional defect. Instead, the structural elements of the RNP that provide selective tRNA−amino acid matching should be explored directly by combined protein and tRNA mutagenesis at the macromolecular interface.

It should also be recognized that protein engineering of bacterial GlnRS to create a misacylating GluRS enzyme has features of a reverse evolutionary trajectory, since a specific Glu-tRNA^{Gln} synthesis activity exists in GluRSND enzymes that were present in the earliest common ancestor of all life (*38*). The mutational experiments presented here simply introduced sequences from the contemporary human GluRS^{D} enzyme and do not represent the reconstruction of an ancestral GlxRS protein using phylogenetic techniques. Such reconstructions in the glucocorticoid receptor system have shown that the pathways of evolutionary development of ligand binding specificity may sometimes not be readily reversed, because intervening epistatic mutations, which generate restrictive structural constraints, limit the capacity of the enzyme to reacquire its ancestral activity (*39*). It is therefore possible that the number of amino acid substitutions ultimately required to fully recreate a highly efficient Glu-tRNA^{Gln} synthesis activity in GlnRS might be quite large, because of a requirement to unravel structural constraints that are not inherently required for the new function.

ACKNOWLEDGMENT

The expression clone for *M. thermautotrophicum* GluRSND was a generous gift from Dieter Söll and Kelly Sheppard.

REFERENCES

1. Ibba, M., and Söll, D. (2000) Aminoacyl-tRNA synthesis. *Annu. Rev. Biochem. 69*, 617–650.
2. Siatecka, M., Rozek, M., Barciszewski, J., and Mirande, M. (1998) Modular evolution of the Glx-tRNA synthetase family: Rooting of the evolutionary tree between the bacteria and archaea/eukarya branches. *Eur. J. Biochem. 256*, 80–87.
3. Woese, C. R., Olsen, G. J., Ibba, M., and Söll, D. (2000) Aminoacyl-tRNA synthetases, the genetic code, and the evolutionary process. *Microbiol. Mol. Biol. Rev. 64*, 202–236.
4. Nureki, O., Vassylyev, D. G., Katayanagi, K., Shimizu, T., Sekine, S., Kigawa, T., Miyazawa, T., Yokoyama, S., and Morikawa, K. (1995) Architectures of class-defining and specific domains of glutamyl-tRNA synthetase. *Science 267*, 1958–1965.
5. Lamour, V., Quevillion, S., Diriong, S., N'Guyen, V. C., Lipinski, M., and Mirande, M. (1994) Evolution of the Glx-tRNA synthetase family:The glutaminyl enzyme as a case of horizontal gene transfer. *Proc. Natl. Acad. Sci. U.S.A. 91*, 8670–8674.
6. Rould, M. A., Perona, J. J., Söll, D., and Steitz, T. A. (1989) Structure of glutaminyl-tRNA synthetase complexed with tRNA^{Gln} and ATP at 2.8 Å resolution. *Science 246*, 1135–1142.
7. Wilcox, M., and Nirenberg, M. (1968) Transfer RNA as a cofactor coupling amino acid synthesis with that of protein. *Proc. Natl. Acad. Sci. U.S.A. 61*, 229–236.
8. LaPointe, J., Duplain, L., and Proulx, M. (1986) A single glutamyl-tRNA synthetase aminoacylates tRNA^{Glu} and tRNA^{Gln} in *Bacillus subtilis* and efficiently misacylates *Escherichia coli* tRNA$_1^{Gln}$ *in vitro*. *J. Bacteriol. 165*, 88–93.
9. Curnow, A. W., Hong, K., Yuan, R., Kim, S., Martins, O., Winkler, W., Henkin, T. M., and Söll, D. (1997) Glu-tRNA^{Gln} amidotransferase: A novel heterotrimeric enzyme required for correct decoding of glutamine codons during translation. *Proc. Natl. Acad. Sci. U.S.A. 94*, 11819–11826.
10. Frechin, M., Duchene, A. M., and Becker, H. D. (2009) Translating organellar glutamine codons: A case by case scenario? *RNA Biol. 6*, 31–34.
11. Sheppard, K., Yuan, J., Hohn, M. J., Jester, B., Devine, K. M., and Söll, D. (2008) From one amino acid to another: tRNA-dependent amino acid biosynthesis. *Nucleic Acids Res. 36*, 1813–1825.
12. Nureki, O., O'Donoghue, P., Watanabe, N., Ohmori, A., Oshikane, H., Araiso, Y., Sheppard, K., Söll, D., and Ishitani, R. (2010) Structure of an archaeal non-discriminating glutamyl-tRNA synthetase: A missing link in the evolution of Gln-tRNA^{Gln} formation. *Nucleic Acids Res.* DOI: 10.1093/nar/gkq605.
13. Schulze, J. O., Masoumi, A., Nickel, D., Jahn, M., Jahn, D., Schgubert, W. D., and Heinz, D. W. (2006) Crystal structure of a non-discriminating glutamyl-tRNA synthetase. *J. Mol. Biol. 361*, 888–897.
14. Skouloubris, S., Ribas de Pouplana, L., de Reuse, H., and Hendrickson, T. L. (2003) A noncognate aminoacyl-tRNA synthetase that may resolve a missing link in protein evolution. *Proc. Natl. Acad. Sci. U.S.A. 100*, 11297–11302.
15. Salazar, J. C., Ahel, I., Orellana, O., Tumbula-Hansen, D., Krieger, R., Daniels, L., and Söll, D. (2003) Coevolution of an aminoacyl-tRNA synthetase with its tRNA substrates. *Proc. Natl. Acad. Sci. U.S.A. 100*, 13863–13868.
16. Uter, N. T., Gruic-Sovulj, I., and Perona, J. J. (2005) Amino acid-dependent transfer RNA affinity in a class I aminoacyl-tRNA synthetase. *J. Biol. Chem. 280*, 23966–23977.
17. Gruic-Sovulj, I., Uter, N. T., Bullock, T. L., and Perona, J. J. (2005) tRNA-dependent aminoacyl-adenylate hydrolysis by a nonediting class I aminoacyl-tRNA synthetase. *J. Biol. Chem. 280*, 23978–23986.
18. Sherlin, L. D., and Perona, J. J. (2003) tRNA-dependent active-site assembly in a class I aminoacyl-tRNA synthetase. *Structure 11*, 591–603.
19. Uter, N. T., and Perona, J. J. (2004) Long-range intramolecular communication in a tRNA synthetase complex examined by chemical quench-flow kinetics. *Proc. Natl. Acad. Sci. U.S.A. 101*, 14396–14401.
20. Bullock, T., Rodriguez-Hernandez, A., Corigliano, E., and Perona, J. J. (2008) A rationally engineered misacylating aminoacyl-tRNA synthetase. *Proc. Natl. Acad. Sci. U.S.A. 105*, 7428–7433.
21. Bullock, T., Uter, N. T., Nissan, T. A., and Perona, J. J. (2003) Amino acid discrimination by a class I aminoacyl-tRNA synthetase specified by negative determinants. *J. Mol. Biol. 328*, 395–408.
22. Hale, S. P., Auld, D. S., Schmidt, E., and Schimmel, P. (1997) Discrete determinants in transfer RNA for editing and aminoacylation. *Science 276*, 1250–1252.
23. Tumbula, D. L., Becker, H. D., Chang, W. Z., and Söll, D. (2000) Domain-specific recruitment of amide amino acids for protein synthesis. *Nature 407*, 106–110.
24. Sherlin, L. D., Bullock, T. L., Nissan, T. A., Perona, J. J., LaRiviere, F., Uhlenbeck, O. C., and Scaringe, S. (2001) Chemical and enzymatic synthesis of tRNAs for high-throughput crystallization. *RNA 7*, 1671–1678.
25. Lyakhov, D. L., He, B., Zhang, X., Studier, F. W., Dunn, J. J., and McAllister, W. T. (1997) Mutant bacteriophage T7 RNA polymerases with altered termination properties. *J. Mol. Biol. 269*, 28–40.
26. Wolfson, A. D., and Uhlenbeck, O. C. (2002) Modulation of tRNA^{Ala} identity by inorganic pyrophosphatase. *Proc. Natl. Acad. Sci. U.S.A. 99*, 5965–5970.
27. Ibba, M., Hong, K. W., Sherman, J. M., Sever, S., and Söll, D. (1996) Interactions between tRNA identity nuclotides and their recognition sites in glutaminyl-tRNA synthetase determine the cognate amino acid affinity of the enzyme. *Proc. Natl. Acad. Sci. U.S.A. 93*, 6953–6958.
28. Kern, D., and LaPointe, J. (1979) Glutamyl transfer ribonucleic acid synthetase from *Escherichia coli*. Study of the interactions with its substrates. *Biochemistry 18*, 5809–5818.
29. Hong, K.-W., Ibba, M., and Söll, D. (1998) Retracing the evolution of amino acid specificity in glutaminyl-tRNA synthetase. *FEBS Lett. 434*, 149–154.
30. Kern, D., Potter, S., Lapointe, J., and Boulanger, Y. (1980) The glutaminyl-transfer RNA synthetase of *Escherichia coli*. Purification,

structure and function relationship. *Biochim. Biophys. Acta 607*, 65–80.
31. Sekine, S., Nureki, O., Shimada, A., Vassylyev, D. G., and Yokoyama, S. (2001) Structural basis for anticodon recognition by discriminating glutamyl-tRNA synthetase. *Nat. Struct. Biol. 8*, 203–206.
32. Madore, E., Florentz, C., Giege, R., Sekine, S., Yokoyama, S., and Lapointe, J. (1999) Effect of modified nucleotides on *Escherichia coli* $tRNA^{Glu}$ structure and on its aminoacylation by glutamyl-tRNA synthetase. *Eur. J. Biochem. 266*, 1128–1135.
33. Sylvers, L. A., Rogers, K. C., Shimizu, M., Ohtsuka, E., and Söll, D. (1993) A 2-thiouridine derivative in $tRNA^{Glu}$ is a positive determinant for aminoacylation by *Escherichia coli* glutamyl-tRNA synthetase. *Biochemistry 32*, 3836–3841.
34. Mukhopadhyay, B., Stoddard, S. F., and Wolfe, R. S. (1998) Purification, regulation, and molecular and biochemical characterization of pyruvate carboxylase from *Methanobacterium thermautotrophicum* strain ΔH. *J. Biol. Chem. 273*, 5155–5166.
35. Rampias, T., Sheppard, K., and Söll, D. (2010) The archaeal transamidosome for RNA-dependent glutamine biosynthesis. *Nucleic Acids Res.* DOI: 10.1093/nar/gkq336.
36. Lipman, R. S., and Hou, Y. M. (1998) Aminoacylation of tRNA in the evolution of an aminoacyl-tRNA synthetase. *Proc. Natl. Acad. Sci. U.S.A. 95*, 13495–13500.
37. Paravisi, S., Fumagalli, G., Riva, M., Morandi, P., Morosi, R., Konarev, P. V., Petoukhov, M. V., Bernier, S., Chenevert, R., Svergun, D. I., Curti, B., and Vanoni, M. A. (2009) Kinetic and mechanistic characterization of *Mycobacterium tuberculosis* glutamyl-tRNA synthetase and determination of its oligomeric structure in solution. *FEBS J. 276*, 1398–1417.
38. Sheppard, K., and Söll, D. (2008) On the evolution of the tRNA-dependent amidotransferases, GatCAB and GatDE. *J. Mol. Biol. 377*, 831–844.
39. Bridgham, J. T., Ortlund, E. A., and Thornton, J. W. (2009) An epistatic ratchet constrains the direction of glucocorticoid receptor evolution. *Nature 461*, 515–520.
40. Uter, N. T., and Perona, J. J. (2004) Long-range intramolecular signaling in a tRNA synthetase complex revealed by pre-steady state kinetics. *Proc. Natl. Acad. Sci. U.S.A. 101*, 14396–14401.
41. Rath, V. L., Silvian, L. F., Beijer, B., Sproat, B. S., and Steitz, T. A. (1998) How glutaminyl-tRNA synthetase selects glutamine. *Structure 6*, 439–449.